JAERI-Research
2002-033



# INFERRING $Z_{eff}$ SPATIAL PROFILE FROM BACKGROUND LIGHT IN INCOHERENT THOMSON SCATTERING DIAGNOSTIC

March 2003

Osamu NAITO and Takaki HATAE

日本原子力研究所
Japan Atomic Energy Research Institute

本レポートは、日本原子力研究所が不定期に公刊している研究報告書です。
入手の問合わせは、日本原子力研究所研究情報部研究情報課（〒319-1195 茨城県那珂郡東海村）あて、お申し越し下さい。なお、このほかに財団法人原子力弘済会資料センター（〒319-1195 茨城県那珂郡東海村日本原子力研究所内）で複写による実費頒布を行っております。

This report is issued irregularly.
Inquiries about availability of the reports should be addressed to Research Information Division, Department of Intellectual Resources, Japan Atomic Energy Research Institute, Tokai-mura, Naka-gun, Ibaraki-ken 〒319-1195, Japan.


編集兼発行　日本原子力研究所

JAERI－Research 2002－033

# Inferring $Z_{eff}$ Spatial Profile from Background Light in Incoherent Thomson Scattering Diagnostic

Osamu NAITO and Takaki HATAE

Department of Fusion Plasma Research
Naka Fusion Research Establishment
Japan Atomic Energy Research Institute
Naka-machi, Naka-gun, Ibaraki-ken

(Received November 1, 2002)

A simulation study on the feasibility of inferring spatial $Z_{eff}$ profile along with electron temperature and density in Thomson scattering diagnostic is presented. The background signal, which is usually discarded after subtracted from the Thomson scattered signal, is used in the reconstruction procedure. If the contribution from line radiation to the background signal is by one order of magnitude smaller than that from bremsstrahlung, a fairly accurate $Z_{eff}$ profile can be reconstructed.

Keywords: Plasma, Incoherent Thomson Scattering, Effective Ionic Charge, Background Light, Bremsstrahlung

# 非協同トムソン散乱計測における背景光データを用いた有効荷電数（$Z_{eff}$）分布の測定

日本原子力研究所那珂研究所炉心プラズマ研究部
内藤　磨・波多江　仰紀

（２００２年１１月　１日受理）

トムソン散乱計測機器を用いて、電子温度分布、電子密度分布と同時にプラズマの有効荷電数（$Z_{eff}$）分布を計測する方法について報告する。通常は正味の散乱光子数を求めるために散乱光からの差し引きだけに使われる背景光のデータは制動放射光の視野積分の情報を含んでいる。シミュレーションによる解析の結果、不純物線からの背景光への寄与が制動放射光の１割以下であれば、この背景光のデータを用いることにより十分な精度で有効荷電数分布を再構成できることを明らかにした。

那珂研究所：〒311-0193　茨城県那珂郡那珂町向山 801-1

## Contents



## 目　次

This is a blank page.

## 1. Introduction

The incoherent Thomson scattering diagnostic [1] is widely used in nuclear fusion research to measure local electron temperature and density of plasma. In this diagnostic, the target plasma is irradiated by a intense laser light and the scattered light, whose spectrum is broadened and shifted toward shorter wavelength, is detected and processed to derive electron temperature and density. The observed scattered light is, however, superposed by background plasma light originating from line radiation and the continuum radiation of bremsstrahlung. To cancel out the effect of background light, data is also taken without the laser radiation and subtracted from the scattered light to yield the net Thomson scattered signal. Usually the measured background light is not used in the inference of electron temperature and density, once subtracted from the scattered light.

The background light has, however, line-integrated information on electron temperature, density, and the effective ionic charge $Z_{eff}$. Therefore in principle it may be possible to infer $Z_{eff}$ profile simultaneously in addition to electron temperature and density. In fact, the measurement of bremsstrahlung radiation in the infrared range using the detection system of Thomson scattering diagnostic was recently conducted and its similarity to the bremsstrahlung radiation in the visible range was reported [2].

However, to make the measurement of $Z_{eff}$ feasible, it is essential to minimize the contribution from line radiation to the background light. In designing the spectrometer of a Thomson scattering system, it is customary to reject major lines in the measured spectrum. Also for the inference of $Z_{eff}$ profile, we can choose only those spectral channels for which the measured spectral widths are narrow and the observed background light is less polluted by line radiation. With all these precautions, there may still be a certain amount of line radiation in the background light. Thus we need to know how much line radiation can be tolerated in the background light so the measurement of $Z_{eff}$ as to be practical. In this report, we present a simulation study on the feasibility of inferring $Z_{eff}$ spatial profile along with electron temperature and density in Thomson scattering diagnostic by utilizing the

background signal consisting of bremsstrahlung and line radiation.

## 2. Reconstruction Method

We assume that the incident wave electric field $\mathbf{E}_i$ is perpendicular to the scattering plane and we measure only the component of scattered wave electric field parallel to $\mathbf{E}_i$. The differential photon cross section per electron per unit solid angle $d\Omega_s$ per unit wavelength shift $\epsilon = (\lambda_s - \lambda_i)/\lambda_i$ can be expressed as [3]

$$\frac{d^2\sigma_p}{d\epsilon d\Omega_s} = q(\epsilon, \theta, 2\alpha)\, r_e^2 \frac{\exp\left(-2\alpha\sqrt{1+\epsilon^2/(2(1+\epsilon)(1-\cos\theta))}\right)}{2K_2(2\alpha)(1+\epsilon)^2\sqrt{\epsilon^2+2(1+\epsilon)(1-\cos\theta)}}, \tag{1}$$

where $\lambda_i$ and $\lambda_s$ are respectively the wavelengths of incident and scattered radiation, $q(\epsilon, \theta, 2\alpha)$ is the depolarization factor [3], $r_e$ is the classical electron radius, $\theta$ is the scattering angle, $2\alpha = m_e c^2/T_e$ with $m_e$, $T_e$, and $c$ being respectively the rest mass and temperature of electron and velocity of light, and $K_2$ is the modified Bessel function of the second kind. Then the total number of Thomson scattering photoelectrons detected on a single spectral channel can be written as

$$N_S = n_e L \Omega_s \frac{\lambda_i U_i}{hc} \int_{\epsilon_l}^{\epsilon_u} \frac{d^2\sigma_p}{d\epsilon d\Omega_s} \eta(\epsilon) T(\epsilon)\, d\epsilon, \tag{2}$$

where $n_e$ is electron density, $L$ is the length of scattering volume, $\Omega_s$ is the solid angle subtended by the collection optics, $U_i$ is the total energy of incident radiation, $h$ is the Planck constant, $\epsilon_u$ and $\epsilon_l$ are respectively the upper and lower bounds of normalized wavelength for this channel, $\eta(\epsilon)$ is quantum efficiency of the detector, and $T(\epsilon)$ is total optical transmission.

The total number of bremsstrahlung photoelectrons collected in a time $\tau$ on a single spectral channel can be written as [4]

$$N_B = dL \sin\theta \Omega_s \tau \int_{s_l}^{s_u} ds \int_{\epsilon_l}^{\epsilon_u} d\epsilon j(\epsilon)\eta(\epsilon)T(\epsilon)\frac{\lambda_i(1+\epsilon)}{hc}, \tag{3}$$

with the spectral power $j(\epsilon)$ emitted into unit solid angle per unit normalized wavelength having the form

$$j(\epsilon) = \frac{8}{3} r_e^3 \frac{m_e c^3}{\lambda_i(1+\epsilon)^2} n_e^2 Z_{eff} \sqrt{\frac{2m_e c^2}{\pi T_e}} \exp\left(-\frac{hc}{T_e \lambda_i (1+\epsilon)}\right) \ln\left(\frac{4T_e \lambda_i (1+\epsilon)\gamma}{hc}\right), \tag{4}$$

where we have adopted the low-frequency Born approximation [4] for the Gaunt factor, $d$ is the diameter of the incident beam, $s$ is a coordinate along the viewing chord with its upper and lower bounds being respectively $s_u$ and $s_l$, and $\gamma$ is Euler's constant.

To infer $T_e$, $n_e$, and $Z_{eff}$, we are to minimize the following $\chi^2$:

$$\chi^2 = \sum_{j=1}^{J}\sum_{k=1}^{K} \frac{(M_{S,jk} - N_{S,jk} - N_{B,jk})^2}{\sigma_{S,jk}^2} + \sum_{j=1}^{J}\sum_{\{k'\}} \frac{(M_{B,jk'} - N_{B,jk'})^2}{\sigma_{B,jk'}^2}, \tag{5}$$

where $M_{S,jk}$ and $M_{B,jk}$ are respectively the measured numbers of scattered (background not subtracted) and background photoelectrons detected on the $k$-th spectral channel of the $j$-th spatial channel, $\sigma_{S,jk}$ and $\sigma_{B,jk}$ are corresponding measurement errors, $J$ and $K$ are numbers of spatial and spectral channels, and $\{k'\}$ denotes the subset of spectral channels used for the inference of $Z_{eff}$. In the ordinary treatment, the following $\chi_j^2$ is minimized for each spatial channel:

$$\chi_j^2 = \sum_{k=1}^{K} \frac{(M_{S,jk} - M_{B,jk} - N_{S,jk})^2}{\sigma_{S,jk}^2 + \sigma_{S,jk}^2}. \tag{6}$$

If we model the $Z_{eff}$ profile by the following rational function

$$Z_{eff}(\rho) = \frac{C_3 + C_4\rho + C_5\rho^2}{1 + C_1\rho + C_2\rho^2}, \tag{7}$$

where $\rho$ is the normalized plasma minor radius, then the parameters to determined are $T_e(\rho_j)$, $n_e(\rho_j)$ ($j$=1,2,$\cdots$,J), and $C_i$ ($i$=1,2,3,4,5).

## 3. Simulation Results

In the following simulation, we assumed a YAG Thomson scattering system with the following specifications: wavelength of incident beam 1064 nm, 10 spatial channels located at $\rho_j = 0.1 \times (j-1)$ ($j$=1,2,$\cdots$,10), scattering angle ranged from 90° ($j = 1$) to 117° ($j = 10$), and 5 spectral channels with their center wavelength and spectral width pairs (in nm) of (1058,6), (1048,15), (1023,35), (958,94), (791,240).

To simulate the measured scattered and background signals, we first calculated the numbers of scattered and bremsstrahlung photoelectrons. The profiles of electron temperature

and density used in this simulation are shown by solid curves in Fig. 1. As for $Z_{eff}$, three test profiles shown by bold curves in Fig. 2 were examined. To mimic the line radiation, 50 to 200 spectral positions were chosen randomly from the spectral range covered by the spectrometer. Then at each spectral position, random number of photoelectrons was added, while the total number of photoelectrons from the line radiation was kept constant for each spatial channel. Now the measured scattered signal corresponds to the sum of photoelectrons from Thomson scattering, bremsstrahlung, and line radiation, and the measured background signal corresponds to the sum of photoelectrons from bremsstrahlung and line radiation. Finally, by adding random Poisson deviates, 32 sets of simulated data $\{M_{S,jk}, M_{B,jk}\}$ were generated and the least squares fittings were carried out using all of the spatial channels ($\{k'\} = \{1, 2, 3, \cdots, K\}$) for the inference of $Z_{eff}$.

We specify the contribution from line radiation by the ratio $I_L/I_B$, where $I_L$ is the total number of photoelectrons from line radiation collected on a certain spatial channel and $I_B$ is that from bremsstrahlung. For the test data used here, the geometrical mean of the signal-to-noise ratio over all spatial and spectral channels was 4.85, when the line radiation was absent, i.e. $I_L/I_B = 0$.

The reconstructed $T_e(\rho)$ and $n_e(\rho)$ inferred with (closed circles) and without (open squares) the background signal are shown in Fig. 1 for the case of $I_L/I_B = 0.1$. We see that using background signal does no harm to the inference of $T_e(\rho)$ and $n_e(\rho)$. In fact, it slightly reduces the error in the inference as shown in Fig. 3. Figure 2 shows the reconstructed $Z_{eff}(\rho)$ for $I_L/I_B = 0.1$ (dashed curves) and $I_L/I_B = 1.0$ (dash-dotted curves). The shaded area shows the uncertainty in the inference. For the case of $I_L/I_B = 0.1$, while the details are not strictly the same, the inferred $Z_{eff}$ profiles are in fair agreement with the true profiles and sufficiently accurate for practical purpose. In contrast, for the case of $I_L/I_B = 1.0$, the absolute value of $Z_{eff}$ is overestimated, even though its approximate peak position can be restored.

To see the effect of line radiation on the inference of $Z_{eff}(\rho)$, we varied $I_L/I_B$ from 0.01 to 2.0. Figure 3 shows the geometrical mean of the relative error in reconstructed

$Z_{eff}$ (bold curve), $T_e$, and $n_e$ over all spatial positions as a function of $I_L/I_B$. The solid and dashed curves correspond respectively to the inferences with and without the use of background signal. Up to $I_L/I_B = 0.1$, existence of line radiation has little effect, probably because the contribution from the line radiation is no larger than the statistical deviation of the background signal. For $I_L/I_B > 0.1$, the inference of $Z_{eff}$ become increasingly worse. Therefore in order that the inference of $Z_{eff}(\rho)$ be feasible, the contribution from line radiation to the background signal should be by one order of magnitude smaller than that from bremsstrahlung. The errors in $T_e$ and $n_e$ are less susceptible to the existence of line radiation, or even a few percent smaller when the background signal is used in the inference.

## 4. Conclusion

In conclusion, if the contribution from line radiation to the background signal is by one order of magnitude smaller than that from bremsstrahlung, we can reconstruct a fairly accurate $Z_{eff}$ spatial profile. In this simulation, all of the spatial channels were incorporated in the inference of $Z_{eff}(\rho)$. But if we select only the channels whose signals are less polluted by line radiation, the inference of $Z_{eff}(\rho)$ will be improved. A drawback of this method is an increased calculation time; for the case presented here, it is about 300 times longer than that of ordinary treatment. Still, with limited resources, e.g. limited number of diagnostic ports, it would be a possible candidate for measuring multiple plasma parameters with a single diagnostic device.

# REFERENCES

[1] J. Sheffield, *Plasma Scattering of Electromagnetic Radiation* (Academic Press, New York, 1975), pp. 191-210.

[2] F. Orsitto, M.R. Belforte, A. Brusadin, E. Giovannozzi, D. Pacella, and M.J. May, Rev. Sci. Instrum. **70**, 925 (1999).

[3] I. H. Hutchinson, *Principles of plasma diagnostics* (Cambridge University Press, Cambridge, 1987), pp. 239-258.

[4] I. H. Hutchinson, *Principles of plasma diagnostics* (Cambridge University Press, Cambridge, 1987), pp. 160-171.

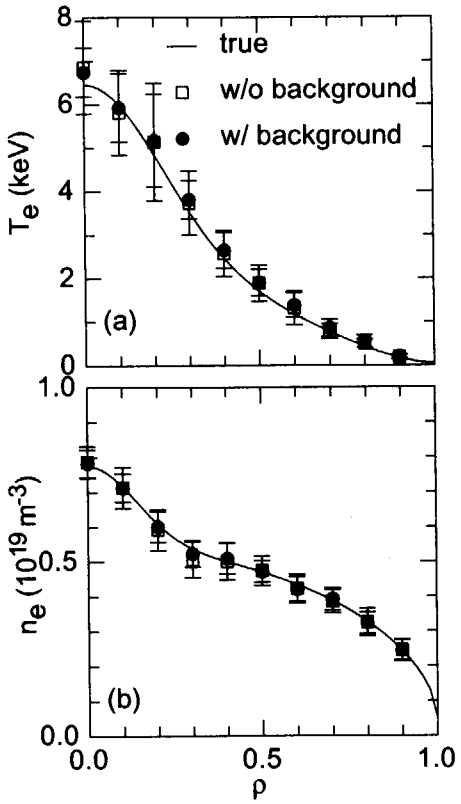


FIG. 1. Profiles of electron (a) temperature and (b) density used in the simulation (solid curves), and the reconstructed profiles with (closed circles) and without (open squares) the use of background signals.

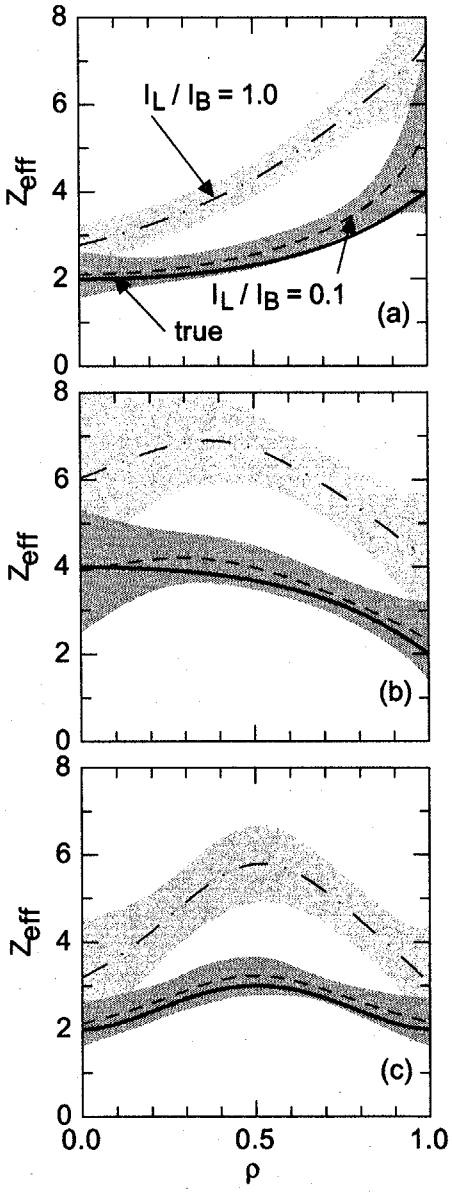


FIG. 2. True (bold curves) and reconstructed (dashed and dash-dotted curves) spatial profiles of effective ionic charge $Z_{eff}$ for three cases. Dashed curves correspond to $I_L/I_B = 0.1$ and dash-dotted curves correspond to $I_L/I_B = 1.0$, where $I_L/I_B$ is the ratio of contribution from line radiation to the background signal to that from bremsstrahlung. Shaded area shows the uncertainty in reconstruction.

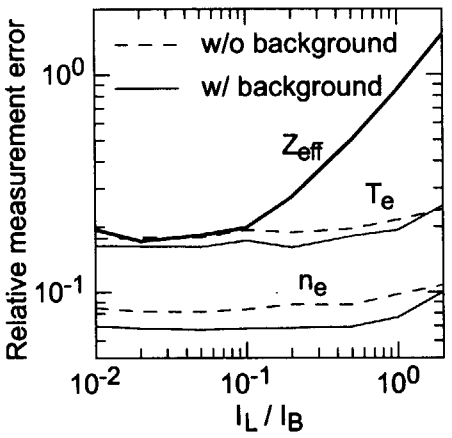


FIG. 3. Mean relative error in inferred $Z_{eff}$ (bold curve), $T_e$, and $n_e$ as a function of $I_L/I_B$. The solid and dashed curves correspond respectively to the inference with and without the background signal.

This is a blank page.

# 国際単位系 (SI) と換算表

**表 1　SI 基本単位および補助単位**

| 量 | 名称 | 記号 |
|---|---|---|
| 長さ | メートル | m |
| 質量 | キログラム | kg |
| 時間 | 秒 | s |
| 電流 | アンペア | A |
| 熱力学温度 | ケルビン | K |
| 物質量 | モル | mol |
| 光度 | カンデラ | cd |
| 平面角 | ラジアン | rad |
| 立体角 | ステラジアン | sr |

**表 2　SI と併用される単位**

| 名称 | 記号 |
|---|---|
| 分，時，日 | min，h，d |
| 度，分，秒 | °，′，″ |
| リットル | l，L |
| トン | t |
| 電子ボルト | eV |
| 原子質量単位 | u |

1 eV = 1.60218 × $10^{-19}$ J

1 u = 1.66054 × $10^{-27}$ kg

**表 5　SI 接頭語**

| 倍数 | 接頭語 | 記号 |
|---|---|---|
| $10^{18}$ | エクサ | E |
| $10^{15}$ | ペタ | P |
| $10^{12}$ | テラ | T |
| $10^{9}$ | ギガ | G |
| $10^{6}$ | メガ | M |
| $10^{3}$ | キロ | k |
| $10^{2}$ | ヘクト | h |
| $10^{1}$ | デカ | da |
| $10^{-1}$ | デシ | d |
| $10^{-2}$ | センチ | c |
| $10^{-3}$ | ミリ | m |
| $10^{-6}$ | マイクロ | μ |
| $10^{-9}$ | ナノ | n |
| $10^{-12}$ | ピコ | p |
| $10^{-15}$ | フェムト | f |
| $10^{-18}$ | アト | a |

**表 3　固有の名称をもつ SI 組立単位**

| 量 | 名称 | 記号 | 他の SI 単位による表現 |
|---|---|---|---|
| 周波数 | ヘルツ | Hz | $s^{-1}$ |
| 力 | ニュートン | N | m·kg/$s^2$ |
| 圧力，応力 | パスカル | Pa | N/$m^2$ |
| エネルギー，仕事，熱量 | ジュール | J | N·m |
| 工率，放射束 | ワット | W | J/s |
| 電気量，電荷 | クーロン | C | A·s |
| 電位，電圧，起電力 | ボルト | V | W/A |
| 静電容量 | ファラド | F | C/V |
| 電気抵抗 | オーム | Ω | V/A |
| コンダクタンス | ジーメンス | S | A/V |
| 磁束 | ウェーバ | Wb | V·s |
| 磁束密度 | テスラ | T | Wb/$m^2$ |
| インダクタンス | ヘンリー | H | Wb/A |
| セルシウス温度 | セルシウス度 | ℃ | |
| 光束 | ルーメン | lm | cd·sr |
| 照度 | ルクス | lx | lm/$m^2$ |
| 放射能 | ベクレル | Bq | $s^{-1}$ |
| 吸収線量 | グレイ | Gy | J/kg |
| 線量当量 | シーベルト | Sv | J/kg |

**表 4　SI と共に暫定的に維持される単位**

| 名称 | 記号 |
|---|---|
| オングストローム | Å |
| バーン | b |
| バール | bar |
| ガル | Gal |
| キュリー | Ci |
| レントゲン | R |
| ラド | rad |
| レム | rem |

1 Å = 0.1 nm = $10^{-10}$ m

1 b = 100 fm$^2$ = $10^{-28}$ m$^2$

1 bar = 0.1 MPa = $10^5$ Pa

1 Gal = 1 cm/$s^2$ = $10^{-2}$ m/$s^2$

1 Ci = 3.7 × $10^{10}$ Bq

1 R = 2.58 × $10^{-4}$ C/kg

1 rad = 1 cGy = $10^{-2}$ Gy

1 rem = 1 cSv = $10^{-2}$ Sv

（注）

1. 表 1 − 5 は「国際単位系」第 5 版，国際度量衡局 1985 年刊行による。ただし，1 eV および 1 u の値は CODATA の 1986 年推奨値によった。
2. 表 4 には海里，ノット，アール，ヘクタールも含まれているが日常の単位なのでここでは省略した。
3. bar は，JIS では流体の圧力を表わす場合に限り表 2 のカテゴリーに分類されている。
4. EC 閣僚理事会指令では bar，barn および「血圧の単位」mmHg を表 2 のカテゴリーに入れている。

## 換　算　表

| 力 | N(=$10^5$ dyn) | kgf | lbf |
|---|---|---|---|
| | 1 | 0.101972 | 0.224809 |
| | 9.80665 | 1 | 2.20462 |
| | 4.44822 | 0.453592 | 1 |

粘度　1 Pa·s(N·s/$m^2$) = 10 P(ポアズ)(g/(cm·s))

動粘度　1 $m^2$/s = $10^4$ St(ストークス)($cm^2$/s)

| 圧力 | MPa(=10 bar) | kgf/$cm^2$ | atm | mmHg(Torr) | lbf/$in^2$(psi) |
|---|---|---|---|---|---|
| | 1 | 10.1972 | 9.86923 | 7.50062 × $10^3$ | 145.038 |
| | 0.0980665 | 1 | 0.967841 | 735.559 | 14.2233 |
| | 0.101325 | 1.03323 | 1 | 760 | 14.6959 |
| | 1.33322 × $10^{-4}$ | 1.35951 × $10^{-3}$ | 1.31579 × $10^{-3}$ | 1 | 1.93368 × $10^{-2}$ |
| | 6.89476 × $10^{-3}$ | 7.03070 × $10^{-2}$ | 6.80460 × $10^{-2}$ | 51.7149 | 1 |

| エネルギー・仕事・熱量 | J(=$10^7$ erg) | kgf·m | kW·h | cal(計量法) | Btu | ft·lbf | eV |
|---|---|---|---|---|---|---|---|
| | 1 | 0.101972 | 2.77778 × $10^{-7}$ | 0.238889 | 9.47813 × $10^{-4}$ | 0.737562 | 6.24150 × $10^{18}$ |
| | 9.80665 | 1 | 2.72407 × $10^{-6}$ | 2.34270 | 9.29487 × $10^{-3}$ | 7.23301 | 6.12082 × $10^{19}$ |
| | 3.6 × $10^6$ | 3.67098 × $10^5$ | 1 | 8.59999 × $10^5$ | 3412.13 | 2.65522 × $10^6$ | 2.24694 × $10^{25}$ |
| | 4.18605 | 0.426858 | 1.16279 × $10^{-6}$ | 1 | 3.96759 × $10^{-3}$ | 3.08747 | 2.61272 × $10^{19}$ |
| | 1055.06 | 107.586 | 2.93072 × $10^{-4}$ | 252.042 | 1 | 778.172 | 6.58515 × $10^{21}$ |
| | 1.35582 | 0.138255 | 3.76616 × $10^{-7}$ | 0.323890 | 1.28506 × $10^{-3}$ | 1 | 8.46233 × $10^{18}$ |
| | 1.60218 × $10^{-19}$ | 1.63377 × $10^{-20}$ | 4.45050 × $10^{-26}$ | 3.82743 × $10^{-20}$ | 1.51857 × $10^{-22}$ | 1.18171 × $10^{-19}$ | 1 |

1 cal = 4.18605 J (計量法)
= 4.184 J (熱化学)
= 4.1855 J (15 °C)
= 4.1868 J (国際蒸気表)

仕事率　1 PS (仏馬力)
= 75 kgf·m/s
= 735.499 W

| 放射能 | Bq | Ci |
|---|---|---|
| | 1 | 2.70270 × $10^{-11}$ |
| | 3.7 × $10^{10}$ | 1 |

| 吸収線量 | Gy | rad |
|---|---|---|
| | 1 | 100 |
| | 0.01 | 1 |

| 照射線量 | C/kg | R |
|---|---|---|
| | 1 | 3876 |
| | 2.58 × $10^{-4}$ | 1 |

| 線量当量 | Sv | rem |
|---|---|---|
| | 1 | 100 |
| | 0.01 | 1 |

(86 年 12 月 26 日現在)

Inferring $Z_{eff}$ Spatial Profile from Background Light in Incoherent Thomson Scattering Diagnostic